Preprint
UCRL-JC-147088

Statistical Stability and Time-Reversal Imaging in Random Media

J. Berryman, L. Borcea, G. Papanicolaou, C. Tsogka

This article was submitted to
Geometric Methods in Inverse Problems and PDE Control,
Minneapolis, MN, July 16-27, 2001

February 5, 2002

U.S. Department of Energy

Lawrence
Livermore
National
Laboratory

Statistical stability and time-reversal imaging in random media

James Berryman* Liliana Borcea† George Papanicolaou‡ Chrysoula Tsogka§

February 5, 2002

Abstract

Localization of targets imbedded in a heterogeneous background medium is a common problem in seismic, ultrasonic, and electromagnetic imaging problems. The best imaging techniques make direct use of the eigenfunctions and eigenvalues of the array response matrix, as recent work on time-reversal acoustics has shown. Of the various imaging functionals studied, one that is representative of a preferred class is a time-domain generalization of MUSIC (MUltiple SIgnal Classification), which is a well-known linear subspace method normally applied only in the frequency domain. Since statistical stability is not characteristic of the frequency domain, a transform back to the time domain after first diagonalizing the array data in the frequency domain takes optimum advantage of both the time-domain stability and the frequency-domain orthogonality of the relevant eigenfunctions.

1 Introduction

There have been many approaches to estimating target location using seismic, ultrasonic, and electromagnetic imaging methods. Some of the most popular ones in recent years continue to be matched-field processing [6, 17], MUSIC (MUltiple SIgnal Classification) [24, 18, 25], and other linear subspace methods [18, 19, 7]. When the targets are imbedded in heterogeneous media so that significant multiple scattering occurs between array and target, the randomness has a different character than that usually envisioned in these traditional analyses. Yet there are a great many applications [11, 12, 13, 14, 10, 27] ranging from the biomedical to ocean acoustics to nondestructive evaluation, where imaging is important and where sources of randomness not associated with the targets to be imaged can play havoc with the traditional methods. Time-reversal acoustics [15, 16, 23] offers part of the answer to these difficult imaging questions, and some significant improvements over these methods for imaging in random media are summarized here.

We have found that methods designed to work well for finding targets in homogeneous media do not necessarily work very well for targets imbedded in random media. In particular, the fact that the linear subspace methods are normally applied in the frequency domain combined with the fact that statistically stable methods are normally found only in the time domain, forces us to seek different imaging strategies in the random media imaging problems of interest to us here. We find that a set of imaging functionals having the desired characteristics exists, and furthermore

*Lawrence Livermore National Laboratories, P. O. Box 808 L-200, Livermore, CA 94551-9900. (berryman1@llnl.gov)

†Computational and Applied Mathematics, MS 134, Rice University, 6100 Main Street, Houston, TX 77005-1892.(borcea@caam.rice.edu)

‡Department of Mathematics, Stanford University, Stanford, CA 94305. (papanico@math.stanford.edu)

§CNRS/LMA, 31 Chemin Joseph Aiguier, 13402 Marseille cedex 20, FRANCE, (tsogka@lma.cnrs-mrs.fr)

that the properties of this set can be completely understood when the time-domain self-averaging — that gives rise to the required statistical stability of the target images — is taken properly into account. We can largely eliminate the undesirable features of the frequency domain methods by making a transform back to the time domain after first diagonalizing sensor array data. While the frequency domain analysis takes optimum advantage of eigenfunction orthogonality of the array data, a transform to the time-domain takes optimum advantage of wave self-averaging which then leads to the statistical stability we require for reliable and repeatable imaging in random media.

In the following sections, we first introduce the imaging problem in the next section. Then we summarize our technical approach. Examples of the cross-range (or bearing) estimates obtained with these methods are presented and then combined with range information from time-delay data to obtain our best estimates and images of target location. The final section summarizes our conclusions about the methods discussed.

2 Imaging Problem

For definiteness, we will treat ultrasonic imaging problems. Our analysis assumes that the array has N transducers located at spatial positions $\mathbf{x}_p$, for $p = 1, \ldots, N$. (See Figure 1.) When used in active mode, the array probes the unknown acoustic medium containing M small scatterers by emitting pulses and recording the time traces of the back-scattered echos. We call the resulting data set the multistatic array response (or transfer) matrix $P(t) = (P_{pq}(t))$, where p and q both range over all the array elements. For our simulations, we consider a linear array where two adjacent point transducers are a distance $\lambda/2$ apart, with λ being the carrier (central) wavelength of the probing pulses. Such an arrangement ensures that the collection of transducers behaves like an array having aperture $a = (N-1)\lambda/2$ and not like separate entities, while keeping the interference among the transducers at a minimum [26]. Our goal is to detect and then localize all M of the targets in the random medium, if possible.

Our simulations assume that $\lambda \leq \ell << a = (N-1)\lambda/2 << L$, where λ is the central wavelength, ℓ is a characteristic length scale of the inhomogeneity (like a correlation length), a is the array aperture, and L is the approximate distance to the targets from the array. This is the regime where multipathing, or multiple scattering, is significant even when the standard deviation of sound speed fluctuations is only a few percent. Values used in the codes are $\lambda = 0.5$mm, $a = 2.5$mm, with a background wave speed of $c_0 = 1.5$km/s. More details concerning the simulations may be found in [5].

Typical array processing methods assume that the targets are far away from the array and, therefore, they look like points. Similarly, the propagation medium is assumed homogeneous and so the observed wavefronts scattered by the targets look like plane waves at the array. Array noise has usually been treated as due either to diffuse sources of white noise coming simultaneously from all directions, or to isolated "noise" having the same types of source characteristics as the targets of interest. But in random media with significant multiple scattering, the resulting "noise" cannot be successfully treated in these traditional ways.

Real-space time-reversal processing of the array response data involves an iterative procedure: sending a signal, recording and storing the scattered return signal, time-reversing and then rebroadcasting the stored signal, with subsequent repetitions. This procedure amounts to using the power method for finding the singular vector of the data matrix having the largest singular value. When the full response/transfer matrix has been measured for a multistatic active array, the resulting data matrix can be analyzed directly by Singular Value Decomposition (SVD) to determine not only the singular vector having the largest singular value, but all singular vectors and singular

values — simultaneously [21, 22, 20].

Imaging is always done using a fictitious medium for the simulated backpropagation that produces these images since the real medium is not known. Its large-scale features could be estimated from other information, such as geological data obtained by seismic methods. For example, migration methods [8, 1, 3] can be used, where very large arrays — much larger than those we contemplate using here — are required. However, the small-scale random inhomogeneities are not known and cannot be effectively estimated, so the simplest thing to do is ignore them when imaging, and use methods that are statistically stable and therefore insensitive to the exact character of these small inhomogeneities.

3 Technical Approach

In our simulations, the array response matrix $\widehat{P}(\omega)$ in the frequency domain is symmetric but not Hermitian. In general (as for array elements with nonisotropic radiation patterns), it is neither Hermitian nor symmetric, but with slight modifications our methods apply to this case as well. The eigenvectors of $\widehat{P}(\omega)\widehat{P}^H(\omega)$ having unit norm are denoted by $\widehat{\mathbf{U}}_r(\omega)$, for $r = 1, \ldots, N$. The eigenvalues of $\widehat{P}(\omega)\widehat{P}^H(\omega)$ are $\sigma_r^2(\omega)$, with $\sigma_r(\omega)$ being the singular values of $\widehat{P}(\omega)$. The significant singular vectors $\widehat{\mathbf{U}}_r(\omega)$ [*i.e.*, those in the range of $\widehat{P}(\omega)$] have singular values $\sigma_r(\omega) > 0$ for $1 \leq r \leq M$, where M is either the number of targets, or the size of the array (N) — whichever is smaller. We assume that the number of targets is smaller than the array size N, so that M is in fact the number of distinguishable targets; this assumption is required by the imaging methods we employ such as MUSIC as will become clear while presenting the method.

The notation used here is the same as in [5]. We denote by $\widehat{\mathbf{g}}_0(\mathbf{y}, \omega)$ the deterministic source vector observed at the array for a source located at $\mathbf{y}^s$. Then, $\widehat{\mathbf{g}}_0(\mathbf{y}, \omega)$ is given by

$$\widehat{\mathbf{g}}_0(\mathbf{y}^s, \omega) = \begin{pmatrix} \widehat{G}_0(\mathbf{y}^s, \mathbf{x}_1, \omega) \\ \widehat{G}_0(\mathbf{y}^s, \mathbf{x}_2, \omega) \\ \vdots \\ \widehat{G}_0(\mathbf{y}^s, \mathbf{x}_N, \omega) \end{pmatrix}, \tag{1}$$

where $\widehat{G}_0(\mathbf{y}^s, \mathbf{x}_j, \omega)$ is the deterministic two-point Green's function, and $\mathbf{x}_j$ is the location of the j-th array element.

We also define the projection $\mathcal{P}_N\widehat{\mathbf{g}}_0(\mathbf{y}, \omega)$ of $\widehat{\mathbf{g}}_0(\mathbf{y}^s, \omega)$ onto the null-space of $\widehat{P}\widehat{P}^H(\omega)$ by

$$\begin{aligned} \mathcal{P}_N\widehat{\mathbf{g}}_0(\mathbf{y}^s, \omega) &= \widehat{\mathbf{g}}_o(\mathbf{y}^s, \omega) \\ &\quad - \sum_{r=1}^{M} \left[\widehat{\mathbf{U}}_r^H(\omega)\widehat{\mathbf{g}}_o(\mathbf{y}^s, \omega) \right] \widehat{\mathbf{U}}_r(\omega), \end{aligned} \tag{2}$$

for each frequency in the support of the probing pulse $\widehat{f}(\omega)$.

The method we describe here is a time domain variant of MUSIC [24, 9], which we label *DOA*, because it gives very stable estimates of the direction of arrival. Frequency domain MUSIC takes a replica (or trial) vector, which is the impulse response or Green's function for a point source at some point in the space, and dots this vector into an observed singular vector at the array. With appropriate normalization, this dot product acts like a direction cosine of the angle between the replica vector and the data vector. If the sum of the squares of these direction cosines is very close to unity, then it is correct to presume that the source point of that replica vector is in fact a target

location since it lies wholely in the range of the array response matrix. Crudely speaking, imaging is accomplished by plotting $1/[1-\cos^2(\cdot)]$, which will have a strong peak when the replica source point is close to the target location.

We form the sum

$$\mathcal{G}^{(j)}(\mathbf{y}^s) = \sum_{p=1}^{N} \left| \mathcal{F}_p^{(j)}\left(\mathbf{y}^s, t_p(\mathbf{y}^s)\right) \right|^2, \tag{3}$$

with

$$\begin{aligned} \mathcal{F}^{(j)}(\mathbf{y}^s, t) &= \int e^{-i\omega t}\sigma_j(\omega)\widehat{\mathbf{g}}_o(\mathbf{y}^s,\omega)d\omega \\ &- \int e^{-i\omega t}\sigma_j(\omega)\sum_{r=1}^{M}\left[\widehat{\mathbf{U}}_r^H(\omega)\widehat{\mathbf{g}}_o(\mathbf{y}^s,\omega)\right]\widehat{\mathbf{U}}_r(\omega)d\omega, \end{aligned} \tag{4}$$

and display the objective functional

$$\mathcal{R}_{\mathrm{DOA}}(\mathbf{y}^s) = \sum_{j=1}^{M} \frac{\min_{\mathbf{y}^s} \mathcal{G}^{(j)}(\mathbf{y}^s)}{\mathcal{G}^{(j)}(\mathbf{y}^s)}, \tag{5}$$

for points $\mathbf{y}^s$ in the target domain.

The arrival time $t_p(\mathbf{y}^s)$ is the deterministic travel time from the p-th transducer to the search point,

$$t_p(\mathbf{y}^s) = \frac{|\,\mathbf{x}_p - \mathbf{y}^s\,|}{c_0}. \tag{6}$$

4 Examples and Range Estimation

Examples for frequency-domain MUSIC with two targets are displayed in Fig. 2. It is clear from this Figure that no range information is obtained from frequency-domain objective functionals, and even the cross-range information is often quite haphazard in random media. Lack of statistical stability prevents these imaging approaches from being useful in random media with significant multipathing as considered here. When the realization of the random medium is changed, the images obtained typically change also — which is what we mean by the phrase "lack of statistical stability" for these methods. Note that this approach works well for homogeneous media, but quickly breaks down when randomness of the velocity field is important.

Examples for time-domain MUSIC with two targets are displayed in Fig. 3. The cross-range results show dramatic improvement over results using other methods [2]. Range information is still not to be found here, due to loss of coherence in the random medium; we cannot get exact cancellation at the targets in this situation whereas coherent refocusing is possible in homogeneous media. But the statistical stability of the universal "comet tails" — which was also anticipated by recent theoretical analyses [4] — is now easily observed. The images are necessarily shown for specific realizations, but the results do not change significantly when the underlying realization of the random medium is changed. This fact has been repeatedly shown in our simulations, and is the main operational characteristic of statistically stable methods.

Target localization requires an estimate of the range. In the far field, only the arrival time information is useful for this purpose. Arrival time information is present in the singular vectors and can also be averaged using multiple copies in the array response matrix for random media —

see [5] — to obtain very stable estimates of arrival times. We will now combine this approach with the time-domain methods to obtain well-localized images of the targets.

For each search point $\mathbf{y}_s$, we compute the objective functional

$$\mathcal{R}_{\mathrm{SAT}}(\mathbf{y}^s) = \sum_{j=1}^{M} \frac{\min_{\mathbf{y}^s} \mathcal{G}^{(j)}_{\mathrm{SAT}}(\mathbf{y}^s)}{\mathcal{G}^{(j)}_{\mathrm{SAT}}(\mathbf{y}^s)}, \tag{7}$$

where

$$\mathcal{G}^{(j)}_{\mathrm{SAT}}(\mathbf{y}^s) = \sum_{p=1}^{N} \left| \mathcal{F}^{(j)}_p(\mathbf{y}^s, t_p(\mathbf{y}^s)) \right|^2 \left[\tau^{(j)}_p - t_p(\mathbf{y}^s) \right]^2. \tag{8}$$

Here $\mathcal{F}^{(j)}(\mathbf{y}^s, t)$ is defined by (4), $t_p(\mathbf{y}^s)$, for $p = 1, \ldots, N$, are the deterministic arrival times given by (6) and $\tau^{(j)}_p$, for $p = 1, \ldots, N$, and $j = 1, \ldots, M$, are the computed arrival times. We call (7) the Subspace Arrival Time (SAT) estimator.

Examples of SAT (or time-domain MUSIC with arrival time estimates from the averaged singular vectors) for two targets are displayed in Fig. 4. This method is statistically stable and gives good estimates of the target locations. These localization results have degraded the least of all those considered [5, 2] at the highest values of the random fluctuations.

5 Conclusions

For imaging applications in randomly inhomogeneous acoustical media, the results summarized here lead us to the following conclusions: (1) Single frequency methods (including MUSIC) are not statistically stable, and therefore cannot be used without modification in the presence of significant amounts of spatial heterogeneity in the acoustic wave speed distribution. (2) In contrast, time domain methods are statistically stable for any objective functional having the characteristic that the random Green's functions appear in Hermitian conjugate pairs of gg^* [5], because large random phases cancel precisely. This result has been shown here to be true for DOA, and is expected to be true more generally. (3) The DOA gives only cross-range information. Range information must be obtained separately.

To isolate the targets in random media, we need either multiple views (using multiple arrays) so we can triangulate, or we need to extract a direct measure of range from the data. In the SAT examples shown here, we used arrival time for the range estimation.

Acknowledgments

Work of J.G.B. performed under the auspices of the U.S. Department of Energy by the University of California Lawrence Livermore National Laboratory under contract No. W-7405-ENG-48 and supported specifically by the LLNL Laboratory Directed Research and Development Program and Environmental Management Sciences Program. The work of L.B. was partially supported by the National Science Foundation under grant number DMS-9971209 and by DOE DE-FG03-00ER25424. The work of G.C.P. was supported by grants AFOSR F49620-01-1-0465, NSF DMS-9971972, DOE DE-FG03-00ER25424, and ONR N00014-02-1-0088.

References

[1] K. Aki and P. G. Richards, *Quantitative Seismology: Theory and Methods*, vol. II, Freeman, New York, 1980.

[2] J. G. Berryman, L. Borcea, G. C. Papanicolaou, and C. Tsogka, *Statisically stable ultrasonic imaging in random media.* currently under review for publication, 2002.

[3] N. Bleistein, J. K. Cohen, and J. W. Stockwell, Jr., *Mathematics of Multidimensional Seismic Imaging, Migration, and Inversion*, Springer, New York, 2001.

[4] P. Blomgren, G. Papanicolaou, and H. Zhao, *Super-resolution in time-reversal acoustics*, J. Acoust. Soc. Am., 111 (2002), pp. 238–248.

[5] L. Borcea, G. C. Papanicolaou, C. Tsogka, and J. G. Berryman, *Imaging and time reversal in random media.* currently under review for publication, 2002.

[6] H. P. Bucker, *Use of calculated sound field and matched-field detection to locate sound sources in shallow water*, J. Acoust. Soc. Am., 59 (1976), pp. 368–373.

[7] M. Cheney, *The linear sampling method and the music algorithm*, Inverse Problems, 17 (2001), pp. 591–596.

[8] J. F. Claerbout, *Fundamentals of Geophysical Data Processing with Applications to Petroleum Prospecting*, McGraw-Hill, New York, 1976.

[9] A. J. Devaney, *Super-resolution processing of multi-static data using time reversal and MUSIC.* to appear in JASA, 2002.

[10] M. Fink, *Chaos and time-reversed acoustics*, Physica Scripta, T90 (2001), pp. 268–277.

[11] ——, *Time reversal acoustics*, Physics Today, 50 (March, 1997), pp. 34–40.

[12] ——, *Time-reversed acoustics*, Scientific American, 281 (November, 1999), pp. 91–97.

[13] M. Fink, D. Cassereau, A. Derode, C. Prada, P. Roux, M. Tanter, J.-L. Thomas, and F. Wu, *Time-reversed acoustics*, Rep. Prog. Phys., 63 (2000), pp. 1933–1995.

[14] M. Fink and C. Prada, *Acoustic time-reversal mirrors*, Inverse Problems, 17 (2001), pp. R1–R38.

[15] M. Fink, C. Prada, and F. Wu, *Self focusing in inhomogeneous media with time reversal acoustic mirrors*, in Proc. IEEE Ultrason. Symp. 1989, B. R. McAvoy, ed., vol. 2, 1989, pp. 681–686.

[16] D. R. Jackson and D. R. Dowling, *Phase conjugation in underwater acoustics*, J. Acoust. Soc. Am., 89 (1991), pp. 171–181.

[17] F. B. Jensen, W. A. Kuperman, M. B. Porter, and H. Schmidt, *Computational Ocean Acoustics*, AIP Press, New York, 1994.

[18] D. H. Johnson, *The application of spectral estimation methods to bearing estimation problems*, Proc. IEEE, 70 (1982), pp. 1018–1028.

[19] D. H. JOHNSON AND S. R. DEGRAAF, *Improving the resolution of bearing in passive sonar arrays by eigenvalue analysis*, IEEE Trans. Acoustics, Speech, Signal Proc., ASSP-30 (1982), pp. 638–647.

[20] N. MORDANT, C. PRADA, AND M. FINK, *Highly resolved detection and selective focusing in a waveguide using the d.o.r.t. method*, J. Acoust. Soc. Am., 105 (1999), pp. 2634–2642.

[21] C. PRADA AND M. FINK, *Eigenmodes of the time reversal operator: A solution to selective focusing in multiple-target media*, Wave Motion, 20 (1994), pp. 151–163.

[22] C. PRADA, S. MANNEVILLE, D. SPOLIANSKY, AND M. FINK, *Decomposition of the time reversal operator: Detection and selective focusing on two scatterers*, J. Acoust. Soc. Am., 99 (1996), pp. 2067–2076.

[23] C. PRADA, F. WU, AND M. FINK, *The iterative time reversal mirror: A solution to self-focusing in the pulse echo mode*, J. Acoust. Soc. Am., 90 (1991), pp. 1119–1129.

[24] R. O. SCHMIDT, *Multiple emitter location and signal parameter estimation*, in Proc. RADC Spectrum Estimation Workshop, Rome, NY, October 1979, Rome Air Development Center, pp. 243–258. RADC-TR-79-63.

[25] ——, *Multiple emitter location and signal parameter estimation*, IEEE Trans. Antennas Propag., AP–34 (1986), pp. 276–281.

[26] B. D. STEINBERG, *Microwave Imaging with Large Antenna Arrays*, Wiley, New York, 1983.

[27] G. TER HAAR, *Acoustic surgery*, Physics Today, 54 (December, 2001), pp. 29–34.

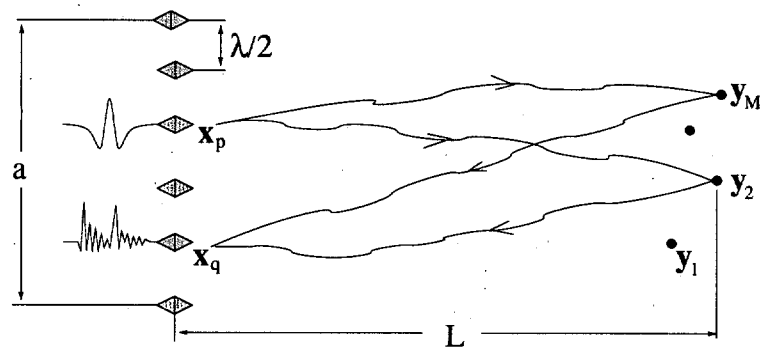

Figure 1: Array probing of a randomly inhomogeneous medium containing M small scatterers.

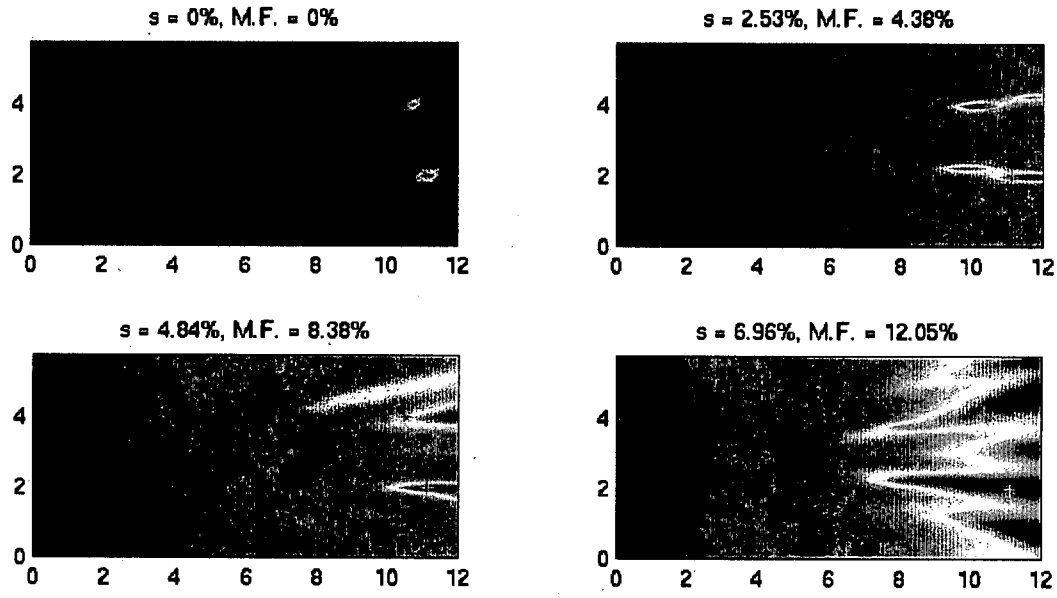

Figure 2: The MUSIC central frequency estimate of the location of two targets in random media with different strength of the fluctuations of the sound speed. The exact location of the targets is denoted by green stars. The standard deviation s and maximum fluctuations (M.F.) are indicated on the top of each view. The horizontal axis is the range in mm and the vertical axis is the cross-range in mm.

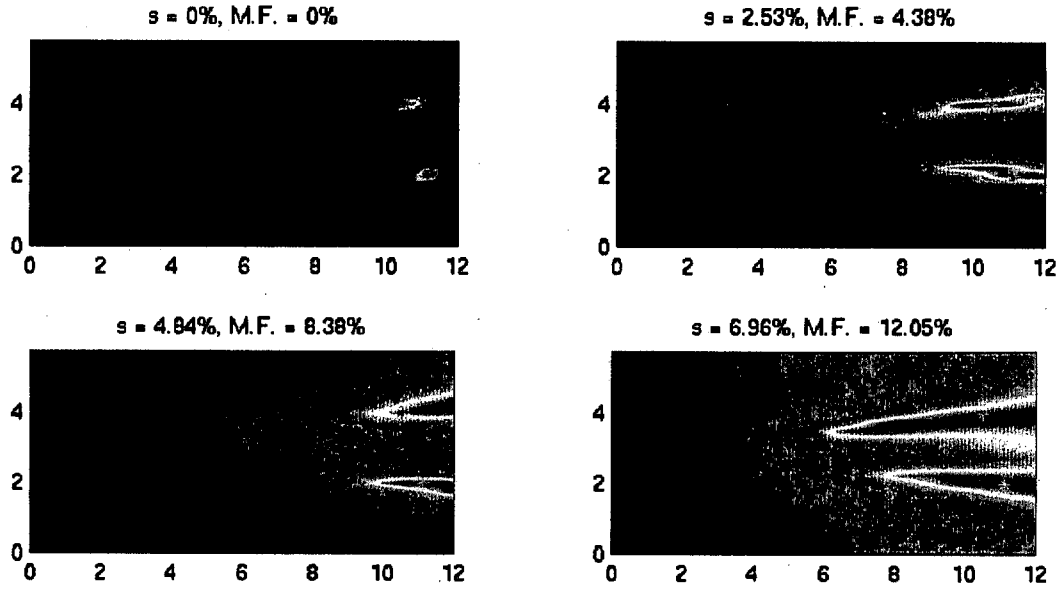

Figure 3: The DOA estimate [*DOA* estimate (5)] of the location of two target in random media with different strength of the fluctuations of the sound speed. The exact location of the target is denoted by the green star. The standard deviation s and maximum fluctuations (M.F.) are indicated on the top of each view. The horizontal axis is the range in mm and the vertical axis is the cross-range in mm.

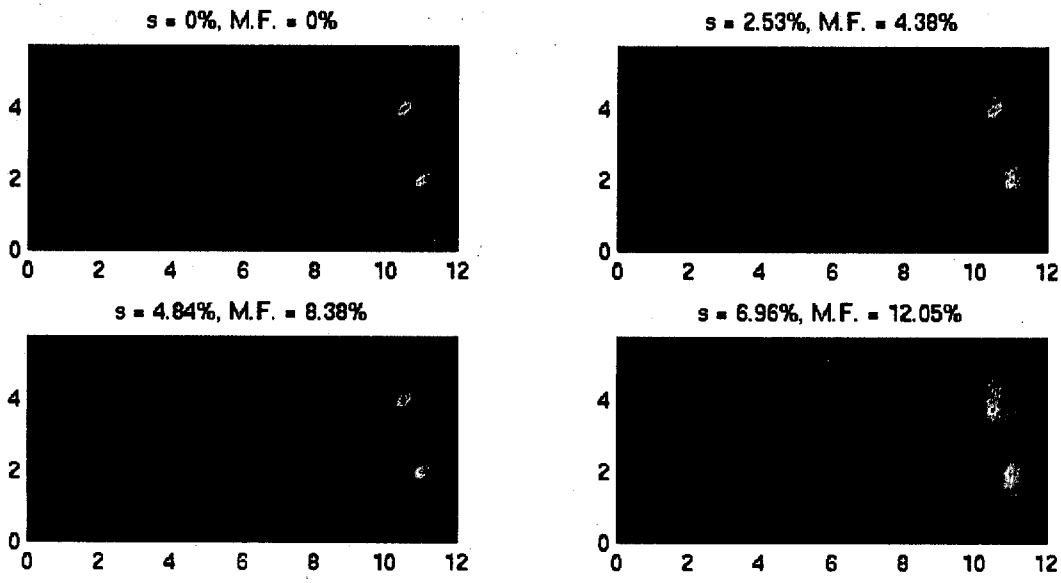

Figure 4: The SAT estimate for two targets.